Integrative Multi-omic Analysis of Human Platelet eQTLs Reveals Alternative Start Site in Mitofusin 2

Lukas M. Simon,[1,2] Edward S. Chen,[2] Leonard C. Edelstein,[3] Xianguo Kong,[3] Seema Bhatlekar,[3] Isidore Rigoutsos,[4] Paul F. Bray,[3,*] and Chad A. Shaw[2,5,*]

Platelets play a central role in ischemic cardiovascular events. Cardiovascular disease (CVD) is a major cause of death worldwide. Numerous genome-wide association studies (GWASs) have identified loci associated with CVD risk. However, our understanding of how these variants contribute to disease is limited. Using data from the platelet RNA and expression 1 (PRAX1) study, we analyzed *cis* expression quantitative trait loci (eQTLs) in platelets from 154 normal human subjects. We confirmed these results in silico by performing allele-specific expression (ASE) analysis, which demonstrated that the allelic directionality of eQTLs and ASE patterns correlate significantly. Comparison of platelet eQTLs with data from the Genotype-Tissue Expression (GTEx) project revealed that a number of platelet eQTLs are platelet specific and that platelet eQTL peaks localize to the gene body at a higher rate than eQTLs from other tissues. Upon integration with data from previously published GWASs, we found that the trait-associated variant rs1474868 coincides with the eQTL peak for mitofusin 2 (*MFN2*). Additional experimental and computational analyses revealed that this eQTL is linked to an unannotated alternate *MFN2* start site preferentially expressed in platelets. Integration of phenotype data from the PRAX1 study showed that *MFN2* expression levels were significantly associated with platelet count. This study links the variant rs1474868 to a platelet-specific regulatory role for *MFN2* and demonstrates the utility of integrating multi-omic data with eQTL analysis in disease-relevant tissues for interpreting GWAS results.

Introduction

Cardiovascular disease (CVD) is a major cause of death worldwide. Thrombotic events, such as myocardial infarction (MI) and stroke, occur when occlusive platelet thrombi form at the site of a ruptured atherosclerotic plaque.[1–5] The critical role of platelets in the pathophysiology of CVD events is further underscored by the standard use of anti-platelet agents in the management of the disease. However, there is little mechanistic understanding to explain why some individuals form occlusive thrombi at the site of ruptured atherosclerotic plaques, whereas other individuals repair the wound without occluding the vessel. Inter-individual variation in platelet reactivity,[6] volume, and number[7] are likely contributors given that these platelet phenotypes have been prospectively shown to be a risk for recurrent coronary syndromes.[8] Abundant evidence suggests that CVD has a genetic component.[9–13] However, the genetic mechanisms underlying CVD risk in the general population are not fully characterized.

Genome-wide associations studies (GWASs) have identified links between CVD risk and genetic variants. However, many disease-associated variants are located in non-coding regions of the genome, making it difficult to identify the mechanism of function.[14–16] Moreover, variations at the DNA level do not pinpoint a tissue of action critical to the development of a higher-level GWAS phenotype such as CVD.[17] Integration of expression quantitative trait loci (eQTLs) from relevant tissues with GWAS results has been proposed as an important approach to overcoming these challenges.[18] eQTLs can provide mechanistic insights into gene expression in disease-relevant tissues by identifying cell-type-specific regulatory variants. Therefore, eQTL data are considered a key intermediate to connecting expression changes with higher-level phenotypes and clinical outcomes represented by GWAS results.[19,20]

Given the role platelets play in the etiology and pathogenesis of CVD, we hypothesized that eQTL analysis in human platelets might connect regulatory variants in platelets with functional expression changes at loci previously linked to CVD by GWASs. Although platelets lack a nucleus, they inherit their transcriptome from their parent bone marrow progenitors, megakaryocytes. Because it is far easier to obtain platelets and because their transcriptome strongly correlates with that of megakaryocytes,[21,22] platelet RNA represents a valuable resource for identifying and characterizing relevant gene expression in thrombotic disorders. We now report a generalizable approach for linking GWAS hits to physiology and disease. This approach integrates cell-type-specific eQTL analysis with primary-tissue multi-omic data from the platelet RNA and expression 1 (PRAX1) study together with other public datasets, such as those of the Genotype-Tissue Expression (GTEx) project[23] and ENCODE.[24] Our analyses and experiments with rs1474868, previously associated with MI by GWASs,[25] revealed that rs1474868 marks the platelet *MFN2* (MIM: 608507) eQTL peak and drives expression of a platelet-specific alternative 5′ start site of *MFN2*. In

addition, we identified a significant association between *MFN2* expression levels and platelet count. Overall, our findings demonstrate the power of integrating primary-tissue eQTL analysis with multi-omic data to interpret and inform functional genomics of GWASs in CVD and other diseases.

Material and Methods

The PRAX1 Study

The goal of the PRAX1 study was to identify gene-expression correlates responsible for inter-individual variation in platelet function. As described earlier,[26,27] 154 healthy individuals (80 of European and 74 of African ancestry) were recruited between 2010 and 2011. For all individuals, demographic information was collected, and platelet functional phenotyping, genome-wide genotyping, and global mRNA profiling were performed. We obtained a complete blood count and mean platelet volume by using an ABX Micros 60 CS (Horiba ABX). Informed consent was obtained from all participants with the approval of the institutional review boards of Baylor College of Medicine in Houston and Thomas Jefferson University in Philadelphia. Research was conducted in accordance with the Declaration of Helsinki.

Gene Expression Data from the PRAX1 Study

We measured gene expression of PRAX1 samples by using the Human Gene 1.0 ST microarray (Affymetrix) as described previously[28] (these data are available in the Gene Expression Omnibus under accession number GEO: GSE49921). eQTL mapping analysis was restricted to 5,695 autosomal, uniquely mapping, commonly expressed platelet mRNAs as defined in Table S1 of Simon et al.[28]

RNA-Seq Data from the PRAX1 Study

A subset of ten subjects from the PRAX1 study were analyzed with RNA-sequencing (RNA-seq) technology in an independent study by Londin et al.[29] (The corresponding next-generation sequencing data files are available in the Sequence Read Archive under study identifier SRA: SRP028846.) Next, we converted raw sequencing files from SOLiD to FASTQ format and trimmed adapters with the "cutadapt" tool. To improve mapping accuracy, we performed a two-pass alignment strategy as outlined in Engstrom et al.[30] First, we used STAR v.2.3.1 to align reads to the UCSC Genome Browser hg19 reference genome. We then used the resulting file on splice junction loci and the hg19 FASTA sequence to generate sample-specific genomes with the –genomeGenerate and –sjdbFileChrStartEnd functions. Reads were subsequently aligned to each sample-specific hg19 index. As mentioned, these RNA-seq data have been previously published, and no global quantification of gene expression was performed for this current study, given that the RNA-seq data were exclusively used in the allelic-imbalance analysis and detailed follow-up analyses of *MFN2* transcription. The RNA-seq data were not used in the eQTL-mapping analysis.

Genotype Data from the PRAX1 Study

DNA from the buffy coats of PRAX1 study subjects was hybridized to the HumanOmni5 array (Illumina) as described earlier[26] and genotyped for approximately five million markers. Genotype data were restricted to 1,927,172 markers passing a cohort-specific minor-allele-frequency cutoff of 5%.

eQTL Mapping

We applied a two-pass eQTL-mapping strategy. First, we used cohort genotype- and microarray-based expression data to identify 612 genes containing at least one significant eQTL association (p < 1e−6, multiple linear regression), termed eGenes. Next, using IMPUTE2 and data from the 1000 Genomes Project, we imputed additional genotypes only for those 612 eGenes. Finally, we repeated association testing by using the extended set of both genotyped (368,794) and imputed (1,071,757) variants to fine map the platelet eQTL landscape of these 612 eGenes. We used R statistical software v.3.0.1 in conjunction with the MatrixEQTL package[31] to determine significant associations between variant-allele dosage and gene expression levels. We restricted the *cis* search space to within 500 kb of the transcription start site and used variant-allele dosage (0, 1, and 2) to additively model associations. The following parameters were used: useModel = modelLINEAR, pvOutputThreshold.*cis* = 1e−6, and cisDist = 5e−5. To account for hidden *trans* covariates, we used the probabilistic estimation of expression residuals (PEER) framework[32] and inferred 15 PEER factors. These PEER factors capture *trans* variation, such as batch effects or global ethnic differences, present in the gene expression data. Accounting for these *trans* factors when modeling *cis* eQTLs improves the power to detect true *cis* eQTLs by reducing spurious false-positive associations.[32] Therefore, we included these 15 PEER factors—in addition to age, gender, and the first two genotype principal components, which completely account for self-identified ethnicity[26]—as covariates in the model. The same settings were used during the first (genotyped variants) and second (genotyped and imputed variants) passes of the eQTL mapping. Significant eQTLs were defined as variants associated with expression levels of genes at a p value threshold of 1e−6 to account for multiple testing. eGenes were defined as genes associated with at least one significant eQTL.

Imputation

To obtain a more granular view of the eQTL landscape, we imputed additional genotypes across the *cis* search space of each eGene prior to the second pass of the eQTL mapping. We used IMPUTE2 v.2.3.2 software[33] and the 1000 Genomes phase 1 integrated variant-set release as a reference to infer additional genotypes. The imputation software first phases the study genotypes and subsequently imputes additional genotypes by integrating study-subject phasing information with known haplotypes from the 1000 Genomes reference data. We followed the instructions provided on the IMPUTE2 website. In short, original genotypes were extracted for each eGene spanning the 1 Mb *cis* search space. Genotypes were pre-phased with the –prephase_g function. We downloaded prephased 1000 Genomes phase 1 integrated haplotypes. Using these pre-phased haplotypes as a reference, we imputed samples from the PRAX1 study with the –use_prephased_g function, for which haplotype and legend files for all 1,092 1000 Genomes samples (246 AFR [African], 181 AMR [admixed American], 286 EAS [East Asian], and 379 EUR [European]) and the PRAX1 study genotype were provided with the –h, –l, and –g parameters, respectively. Imputed genotypes called with high confidence (maximum probability > 0.9) were used in subsequent analysis. Accuracy analysis was performed with the IMPUTE2 internal cross-validation system. During each run, IMPUTE2 masks a subset of observed variants and subsequently imputes these genotype data by using flanking markers. The imputation accuracy can be quantified as the percentage of concordance between known and imputed genotypes of these

cross-validated variants. In the cross-validation analyses, the percentage of concordance across the 612 eGene regions was very high (minimum = 96.4%, median = 98.7%, maximum = 99.7%), indicating accurate imputation results. Because of the nature of overlapping *cis* search spaces, some variants were imputed multiple times. In these cases, imputed genotypes with discordant results were excluded.

Conditional eQTL Analysis

To investigate how many independent eQTL signals contribute to the regulation of a single eGene, we performed conditional eQTL analysis. This analysis followed the procedures outlined in the eQTL Mapping section, but additionally, the genotype of the marker for the corresponding eQTL peak was added as a covariate for each of the 612 eGenes. If no variants remained significantly associated with expression of the corresponding eGene (p < 1e−6) after we accounted for the genotype of the marker at the eQTL peak, we defined the given eGene as regulated by a single genetic signal. If a significant association remained, we interpreted it as evidence of a second independent genetic signal.

Analysis of Allele-Specific Expression

We analyzed allele-specific expression (ASE) with our ten RNA-seq samples from the PRAX1 study. Using the reference genome to map RNA-seq data can be biased by genetic variation, given that reads carrying the non-reference allele are less likely to map correctly.[34] This mapping bias is called reference-allele bias and is a non-trivial confounding variable in ASE analysis.[35] To overcome this challenge, we aligned RNA-seq reads to inferred personalized genomes on the basis of the genotype data observed in the study. This specialized alignment was used in the ASE analysis only. To generate personalized genomes corresponding to the ten RNA-seq samples from the PRAX1 study, we used IMPUTE2 v.2.3.2 to impute genotypes across 22 autosomal chromosomes (as outlined in the Imputation section); this procedure generates a high-density map of the personal variation present in each sample. Following the recommendations on the IMPUTE2 website regarding the imputation of entire chromosomes, we divided each chromosome into 500 kb intervals and imputed each interval separately. Phasing information obtained from the imputation can be used for inferring parental haplotypes across genetic regions, such as genes. We used the "vcf2diplod" function provided in the AlleleSeq[36] software to generate two paternal-genome FASTA files for each sample. Next, we used the –genomeGenerate parameter of STAR v.2.3.1 to generate two separate parental-genome indices for each sample. Because of imputed insertion and deletions, the "liftOver"[37] function was needed to convert genomic coordinates between genomes. Next, for each sample, we used STAR v.2.3.1 to align the corresponding FASTQ read file to the two paternal genomes independently. Figure S1 shows that reference-allele bias decreased when RNA-seq reads were aligned to personalized genomes rather than the hg19 reference genome. Next, read pileups were generated with an adapted version of the pipeline outlined in Harvey et al.[38] In short, SAMtools[39] was used to generate read pileups at 128,163 (genotyped and imputed) sites, which were used in the eQTL-mapping analysis and fell into coding regions according to the UCSC Genome Browser hg19 knownGene table downloaded in January 2015. Next, heterozygous sites within each of the ten PRAX1 study samples were identified and assessed for coverage. Heterozygous coding sites with ten or more reads in a sample were required for the site to be considered in the ASE analysis. To ensure that map-ping bias did not affect the calculations, we calculated and recorded the pair of counts for each parental allele from the alignment to the corresponding personalized parental genome. Because a gene can harbor more than one heterozygous coding site in a given sample, we picked the pileup site with the lowest eQTL association p value to examine allelic imbalance. Allelic imbalance was defined as an unequal count of two alleles at a given heterozygous pileup site in a sample. To evaluate the global correspondence between allelic imbalance and the genome-wide global eQTL findings, we used Fisher's exact test. The null hypothesis states that the directionality of allelic imbalance is independent of the allelic directionality of the eQTL. In other words, the likelihood of observing a higher fraction of the reference allele than of the alternative allele at a given pileup site is independent of the allele implicated with higher expression levels in the eQTL analysis. Directional deviation from this null hypothesis would indicate concordance between allelic imbalances and eQTLs. For the exemplary eGene *CXCL5*, we developed a separate statistical approach. In order to give equal weight to each sample, we downsampled allelic counts of each heterozygous sample to the minimum sum of allelic counts among all heterozygous samples. Next, we summed these counts into an aggregate pair of counts and performed a binomial test. The null hypothesis for this test states that the likelihoods of observing the reference and alternative alleles are equal, so that reads are generated as coin-flipping trials of a fair coin. Appropriate deviation from this null hypothesis can indicate that allelic imbalance corresponds to the allelic directionality of the eQTL; p values were determined for a one-sided binomial test.

GTEx Data

These data consist of a resource database and associated tissue bank for studying the relationship between genetic variation and gene expression in human tissues. We downloaded the GTEx_Analysis_V6_eQTLs.tar.gz table, containing significant single-tissue variant-gene associations from the GTEx website. These data catalog eQTLs across 46 different tissues. To increase comparability, we restricted analysis to 20 GTEx tissues with a sample size equal to or higher than our PRAX1 study cohort (154) and redefined all GTEx eGenes according to our definition: GTEx eGenes for each tissue were defined as genes containing at least one significant eQTL (p < 1e−6) within 500 kb of the transcription start site. Our definition of an eGene was more stringent than the rules applied by GTEx. Across the 20 tissues analyzed, on average, a subset of 71% of GTEx eGenes remained an eGene according to our definition. An eQTL peak was defined as the genomic location of the most strongly associated eQTL variant(s) within each eGene. Table S3 lists eQTL peaks for GTEx and platelet eGenes. To account for varying sample sizes inherent in the GTEx eQTL dataset, we used Jaccard similarity to compare overlap between platelet and GTEx eGenes. To perform a more granular comparison, we conducted an additional analysis at the variant-gene association level. For each eGene we identified the strongest platelet eQTL association present in each of the GTEx tissues. Next, we compared the sign of the allelic effect of the eQTL association. Concordance between the sign of the allelic effects of eQTL associations in platelets and each GTEx tissue was calculated with Fisher's exact test. The null hypothesis is that the sign of the allelic effect of the eQTL in platelets is independent of the sign of the allelic effect in the tissue of comparison. Directional deviation from this hypothesis can indicate concordance of allelic effects between the tissues at the variant-gene level.

CVD GWAS Associations

We used the Phenotype-Genotype Integrator[25] to download previously published GWAS results. We restricted analyses to variants associated with traits annotated to the Medical Subject Headings (MeSH) category "cardiovascular diseases" and an association p value below 1e−4. These data catalog variant-phenotype associations and were integrated with the variant-eGene associations identified in our eQTL analysis.

Additional Platelet RNA-Seq Data

We downloaded additional platelet RNA-seq data from three previous studies by Rowley et al.,[40] Kissopoulou et al.,[41] and Eicher et al.[42] For the Rowley et al. data, RNA-seq alignments were downloaded according to the instructions outlined in Rowley et al.[40] For the Kissopoulou et al. data,[41] next-generation sequencing FASTQ files were downloaded from the ArrayExpress website under accession number E-MTAB-1846. Reads were aligned to the hg19 reference genome with STAR v.2.3.1 using default parameters. For the Eicher et al. data,[42] next-generation sequencing FASTQ files and corresponding metadata were downloaded from study SRP053296 in the Sequence Read Archive. Sample runs SRR1792698 and SRR1792703 contained errors in the read-pairing annotation and were excluded from further analysis. Reads were aligned to the hg19 reference genome with STAR v.2.3.1 using default parameters. These data comprise RNA-seq data from different library-preparation protocols (total RNA, polyA, and rRNA depleted) and sequencing technologies (Illumina and SOLiD). Using data produced by different groups via different techniques and protocols to validate RNA-seq-based findings limits the chance of false-positive associations due to technical artifacts of the sequencing pipeline. Therefore, we used these independent observations as evidence supporting the expression of exon 2b in platelet *MFN2* and an increase in sample size for associative analyses.

In Silico Cross-Tissue Analysis

The Epigenome Roadmap project contains mRNA-seq data from stem cells and primary ex vivo tissues selected to represent the normal counterparts of tissues and organ systems frequently involved in human disease. We used the Genboree Workbench[43] to analyze mRNA-seq expression data for the *MFN2* region from 69 samples. As input, we provided a customized bed file of 10 bp intervals spanning the *MFN2* region. Using this file, we calculated average read density per interval for each sample. Replicates within a sample type were averaged. Read-density averages across these intervals for all samples can be found in Table S4.

PCR Confirmation of *MFN2* Exon 2b

Leukocyte-depleted platelet RNA (henceforth referred to as "platelet RNA") was obtained via density centrifugation and immune depletion of CD45^{+} cells as described previously.[44] 500 ng of platelet RNA and SuperScript III (ThermoFisher Scientific) were used for cDNA generation. PCR was performed to amplify and detect the presence of the canonical *MFN2* sequence (GenBank: NM_014874.3) spanning exons 1–3 (primers F1 and R1), the platelet *MFN2* sequence spanning exons 2b and 3 (primers F2 and R2), and exons 7–10 in *ITG2B* as a positive control for RNA quality (primers *ITG2B*-F and *ITG2B*-R). The primer sequences were as follows: 5′-GGTGACGTAGTGAGTGTGATG-3′ (F1), 5′-CACTTAAGCACTTTGTCACTGC-3′ (R1), 5′-CCCAGCTGACCTGTTTATTTG-3′ (F2), 5′-CTACATCCAGGAGAGCGC-3′ (R2), 5′-AGA

GTACTTCGACGGCTACTG-3′ (*ITG2B*-F), 5′-GCAGCCTCTGGTAG TAGGAA-3′ (*ITG2B*-R).

5′ Rapid Amplification of cDNA Ends of *MFN2*

To map the definitive 5′ end of the platelet *MFN2* transcript, we used the SMARTer RACE (5′ rapid amplification of cDNA ends) 5′/3′ Kit (Clontech) as described by the manufacturer. In brief, 1 μg platelet RNA was used for synthesis of first-strand cDNA, which added a universal priming sequence to the 5′ end of the first strand via template switching. The 5′ end of the cDNA was then amplified in two rounds of nested PCR using primers that anneal to the universal priming sequence (provided by the manufacturer) and two gene-specific primers: 5′-CACTTAAGCACTTTGTCA CTGC-3′ (GSP-1) and 5′-CGGGTAGAGGGCACAGATGGCCAT GAGG-3′ (GSP-2). The products of the second round of amplification were run on an agarose gel cloned into the pRACE vector with the provided In-Fusion HD Cloning Kit. The cloned products were then sequenced.

Relative Abundance of *MFN2* Isoforms

The relative abundance of *MFN2* isoforms was calculated with the splice-loci output generated from the STAR alignments for the RNA-seq data from the PRAX1 study, Kissopoulou et al., and Eicher et al. To estimate the relative abundance of the *MFN2* isoform containing exon 2b, we calculated the number of spliced reads that mapped from the 3′ border of exon 2b (chr1: 12,044,353, hg19) to the 5′ border of exon 3 (chr1: 12,049,221, hg19) and divided it by the number of all spliced reads ending at the 5′ border of exon 3. Samples with ten or fewer junction reads ending at the 5′ border of exon 3 were excluded.

Inference of rs1474868 Genotype

Because the variant rs1474868 falls into a coding region, we were able to infer the rs1474868 genotype by using the STAR alignments for the Kissopoulou et al.[41] and Eicher et al.[42] data. Samples with more than one read containing the C or T allele were assigned the corresponding genotype. Samples with a total of fewer than two reads were assigned the unknown status.

Transcription Factor Binding Sites

ENCODE chromatin immunoprecipitation followed by sequencing (ChIP-seq) data on transcription factor binding were downloaded from UCSC Genome Browser. We subsequently restricted all data to experiments carried out in the hematopoietic-derived K562 cells.

MFN2 Luciferase Assays

DNA from two PRAX1 study subjects homozygous for C or T at SNP rs3766744 was used as a template for amplifying two regions surrounding this SNP: (1) a 655 bp region (chr1: 12,043,332– 12,043,986, hg19) was amplified with primers 5′-GTTAGCC AGGATGGTCTCGAAC-3′ and 5′-AACTTGCAAGCTGAGATTC CAC-3′, and (2) a 1,928 bp region (chr1: 12,042,341–12,044,268, hg19) was amplified with primers 5′-TTCGCTGGTTGCTTAGA GAG-3′ and 5′-AAGTTCCCTGCCATCAGAAG-3′. The amplified fragments were then cloned upstream of a basal promoter in the pGL4.28-luc vector (Promega). A total of four vectors were produced: *MFN2*:655(C)-Luc, *MFN2*:665(T)-Luc, *MFN2*:1928(C)-Luc, and *MFN2*:1928(T)-Luc. 2 μg of a *MFN2*-Luc vector was transfected along with 0.5 μg CMV-β-gal-expressing plasmid into 5 × 10^{5} K562 cells. 24 hr after transfection, lysates were measured for
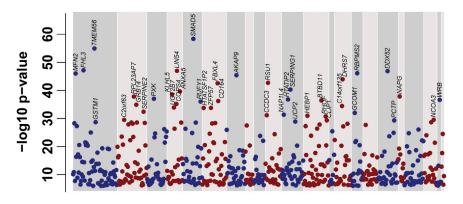
Figure 1. Genome-wide View of Platelet eGenes
The y axis shows maximum $-\log_{10}$ p values of eQTLs for 612 platelet eGenes. The x axis corresponds to ordering along 22 autosomal chromosomes. The top 40 eGene symbols have been added to the plot. Color coding of points and backgrounds is used to help separate chromosomes visually.

luciferase activity on a FLUOstar OPTIMA plate reader (BMG Labtech) and β-gal activity with a beta-Galactosidase Assay Kit (ThermoFisher). Results are expressed as a ratio of luciferase activity normalized to β-gal activity.

Statistical Analyses

Statistical analyses were conducted with R statistical software. To evaluate the significance of differences in the distribution of eQTL peaks between platelets and GTEx tissues, we performed the Grubbs single-outlier test on the proportion of eQTL peaks mapping into the gene body by using the "grubbs.test" function from the "outliers" R package. We used Spearman's rank correlation to assess significance between the exon 2b inclusion rate and rs1474868 allele dosage. We used Mann-Whitney tests as implemented in the "wilcox.test" R function to evaluate significance of differential luciferase activity. We used the LDlink online tool to assess linkage disequilibrium. To best represent our study cohort, we restricted linkage-disequilibrium calculations to the 1000 Genomes populations ASW (Americans of African ancestry in southwest USA) and CEU (Utah residents with ancestry from northern and western Europe from the CEPH collection). We used a multiple-linear-regression framework implemented in the R "aov" function to evaluate the significance of the association among platelet count, the rs3766744 genotype, and *MFN2* expression levels in the PRAX1 study data. For the rs3766744 variant, the model explained platelet count by using rs3766744 allele dosage after accounting for the marginally significant covariates body mass index, gender, and self-identified ethnicity. For *MFN2* expression levels, the model explained platelet count by using *MFN2* expression levels after accounting for the same covariates.

Results

Two-Pass *cis* eQTL Mapping Identifies 612 Platelet eGenes

The PRAX1 study profiled mRNA expression levels from platelets and genotypes of 154 healthy human subjects on array platforms.[26] To decrease computational burden while increasing genetic resolution, we applied a two-pass strategy for mapping the landscape of human platelet *cis* eQTLs (see Material and Methods). 5,695 autosomal commonly expressed platelet genes, as defined in Simon et al.,[28] were used in the analysis. We identified a total of 44,940 significant eQTLs ($p < 1e-6$) implicated in expression association with 612 unique genes, termed platelet

eGenes. The rates of the number of eGenes per gene tested and significant eQTLs per eGene were comparable to those of other studies with similar sample sizes (Figure S2). Figure 1 presents the distribution of the strongest association p values for each eGene across the 22 autosomal chromosomes tested. To assess how many eQTLs contribute to the association signal of an eGene, we performed conditional eQTL analysis. 560 (92%) eGenes did not contain any significant eQTLs after we accounted for the eQTL peak, indicating that most platelet eGenes are regulated by a single genetic signal. The MatrixEQTL output for all 612 platelet eGenes is contained in Table S1. These results can be interactively queried on our Plateletomics website (see Web Resources).

ASE Analysis Confirms Global eQTL Results In Silico

An eQTL measures the association between genotype and gene expression across samples, whereas ASE measures allelic imbalance at a heterozygous site within a single sample.[45] Concordance between the allelic directionality of allelic imbalance and an eQTL can be interpreted as an independent validation of the eQTL.[46] Figure S3 contains a detailed schematic describing the relationship between eQTLs and ASE. Therefore, we performed allelic-imbalance analysis (see Material and Methods). In brief, to validate eGenes by using allelic imbalance, we generated read pileups at heterozygous coding sites of all platelet eGenes in all ten RNA-seq samples from the PRAX1 study. A total of 116 (19%) eGenes contained at least one qualifying pileup site with marginal eQTL effect ($p < 1e-4$) in one or more of the ten samples and provided the opportunity to confirm eQTL effects via allelic-imbalance analysis. We classified all pileup sites of these 116 eGenes according to the allelic directionality of the linked eQTL. Reference and alternatives sites were defined as pileup sites where the linked eQTL showed higher expression of the reference and alternative allele, respectively.

Figure 2A presents the counts of reference and alternative alleles observed at 358 pileup sites corresponding to 116 unique eGenes (Table S2). 266 (75%) alternative and reference sites fell above and below the diagonal line, respectively. The allelic imbalances are in concordance with the allelic directionality of the eQTLs and
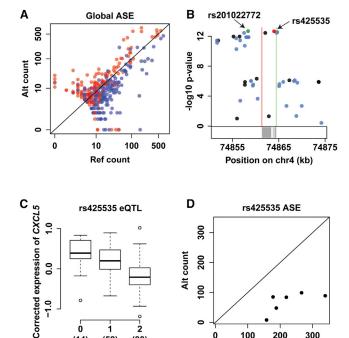
Figure 2. Confirmation of eQTLs via ASE

(A) Points represent allele counts at 358 heterozygous coding sites with a marginal eQTL effect (p < 1e−4). Reference and alternatives sites are colored in blue and red, respectively. The black diagonal line indicates the null-hypothesis distribution of equal counts of the reference and alternative alleles.

(B) Manhattan plot of eQTL landscape for eGene *CXCL5*. The y and x axes correspond to association p values and genomic coordinates, respectively. Blue and black points show imputed and genotyped variants, respectively. The red point shows reference site rs425535, and the green point shows lead eQTL rs201022772. Transcription start and end sites of *CXCL5* are indicated by green and red vertical lines, respectively. Gray rectangles below the plot represent *CXCL5* exons.

(C) Boxplot shows significant association between *CXCL5* expression levels and rs425535 allele dosage (p < 10e−12, multiple linear regression).The x axis shows the alternative allele count. Numbers in parentheses indicate the number of samples within each group. The y axis represents expression levels of *CXCL5* corrected for covariates. The box represents the interquartile range, the horizontal line in the box indicates the median, and the whiskers represent 1.5× the interquartile range.

(D) Reference and alternative allele counts at rs425535 for six heterozygous RNA-seq samples from the PRAX1 study are shown on the x and y axis, respectively.

demonstrate the agreement between eQTLs and ASE (p < 1e−19, Fisher's exact test).

Figures 2B–2D depict *CXCL5* (MIM: 600324), a representative eGene. *CXCL5* was chosen because it shows significant allelic imbalance in concordance with the allelic directionality of the eQTL (p < 2.2e−16, binomial test; see Material and Methods for additional details). CXCL5 is a neutrophil-recruiting chemokine that is secreted by platelets. Platelet-released CXCL5 participates in the pathogenesis of coronary artery disease and tumor metastases.[47,48] The Manhattan plot in Figure 2B shows the eQTL landscape of *CXCL5*. The reference site rs425535 (red point) is in the second exon of the gene and was in

linkage disequilibrium with the lead eQTL rs201022772 (green point). High *CXCL5* expression levels were associated with the reference allele of variant rs425535 (p < 10e−12, multiple linear regression; Figure 2C). Correspondingly, ASE analysis at rs425535 revealed a higher proportion of the reference allele within all six heterozygous samples (Figure 2D). We interpret these results as in silico ASE validation of the eGene *CXCL5*.
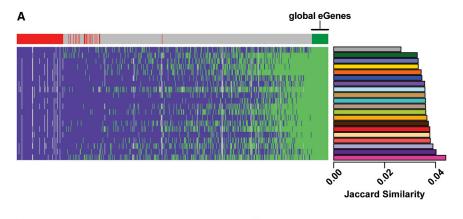
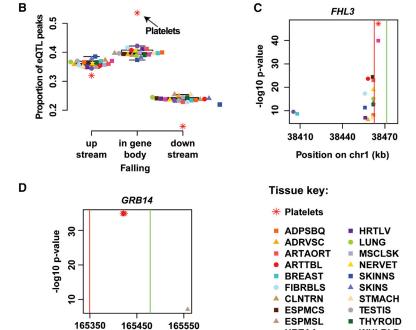**Platelets Share eGenes with Other Tissues**

To compare our platelet eQTLs to those identified in other tissues, we reanalyzed GTEx eQTL data[23] from 20 different tissues isolated from human cadavers. To improve comparability, we applied our definition of eGenes to the GTEx data (Material and Methods; Table S3). 525 platelet eGenes (86%) were also identified as eGenes in at least one of the GTEx tissues analyzed (p < 2.2e−16, binomial test), additionally validating our eQTL results. To investigate eGenes at a higher resolution, we compared variant-gene associations of our platelet eQTLs to corresponding variant-gene associations tested in the GTEx data. We observed a 75% median concordance rate for the sign of the effect between platelet eQTLs and GTEx tissues, indicating that eGenes commonly share the allelic directionality of their eQTLs (median p value across tissues < 1e−6, Fisher's exact test; Figure S4). 33 platelet eGenes were classified as eGenes in all 20 GTEx tissues and were therefore considered global eGenes. To evaluate overlap between platelet eGenes and each GTEx tissue separately, we calculated Jaccard similarity. The GTEx tissue "whole blood" shared the highest fraction of eGenes with platelets (258 common eGenes). A total of 110 platelet eGenes were identified as platelet specific because they were observed exclusively in platelets, exempting the GTEx tissue "whole blood," of which platelets are a component (Figure 3A).

Platelet eQTL Peaks Tend to Localize in the Gene Body

To examine eGenes at a more granular level, we defined eQTL peaks as the genomic location of the variant(s) with the strongest association with a given eGene. We identified all eQTL peaks in platelets and GTEx tissues independently. When we compared eQTL peaks to the eGene's transcription start and stop sites across tissues, platelets had an unusually large proportion of eQTL peaks (54%) mapping to the gene body (p < 1e−8, Grubbs single-outlier test; Figure 3B). This finding suggests that anucleate platelets might be subjected to an expression-regulation architecture that is distinct from that of other tissues with active transcription.

When both GTEx data and platelets have eQTLs for the same eGene, a variety of patterns can emerge. We highlight two exemplary eGenes, such as *FHL3* (MIM: 608898), known to play a role in platelet biology. Platelets require Munc13-4 for granule fusion and release,[49] and mutations in *FHL3* cause defective secretion and familial hemophagocytic lymphohistocytosis.[50] Figure 3C depicts

Figure 3. Comparison of Platelet eQTLs with GTEx

(A) Heatmap columns and rows represent platelet eGenes and GTEx tissues, respectively. The color of the heatmap represents the classification of each platelet eGene as either an eGene (green) or not an eGene (purple) in each of the GTEx tissues. Gray colors indicate genes not tested for eQTLs in the given tissue. In the bar above the heatmap, green and red represent global and platelet-specific eGenes, respectively, and gray indicates platelet eGenes co-occurring in one or more GTEx tissues. The adjacent barplot shows Jaccard similarity comparing the overlap between platelet eGenes and GTEx tissues.

(B) The relative distribution of eQTL peaks across the gene body for all tissues. The box represents the interquartile range, the horizontal line in the box indicates the median, and the whiskers represent 1.5× the interquartile range.

(C and D) The location of eQTL peaks for eGenes *FHL3* and *GRB14*. The y and x axes correspond to the $-\log_{10}$ p value of eQTL peaks and genomic location, respectively. Green and red vertical lines illustrate the transcription start and stop sites, respectively, for each gene.

the eQTL peaks for the eGene *FHL3* across studies. A cluster of eQTL peaks mapped just downstream of the transcription stop site (red vertical line) in multiple tissues, and eQTL peaks fell even further downstream in "heart-atrial appendage" and "breast-mammary tissue." However, the eQTL peaks for platelets (red asterisk) and the GTEx tissue "whole blood" (purple square) overlapped each other and mapped, distinct from the other GTEx tissues, into the gene body. This observation suggests that the molecular regulation underlying *FHL3* expression might be similar in platelets and blood and different from that in other tissues.

Figure 3D depicts the eQTL peaks for an additional exemplary platelet eGene *GRB14* (MIM: 601524), which encodes growth factor receptor-bound protein 14. This protein is an adaptor that regulates receptor tyrosine kinase signaling, platelet signaling, and integrin activation.[51] The platelet eQTL peak localized to the gene body, whereas in the GTEx tissue "esophagus muscularis," the eQTL peak fell upstream of the gene.

Overlap between Platelet eQTL Peaks and MI Variants in *MFN2*

To assess our eQTL findings in the context of CVD GWAS results, we systematically compared our eQTL findings to data from the Genotype and Phenotype Integrator.[25] A total of 3,850 unique variants were previously reported to be associated with the risk of CVD in various studies at a p value threshold of 1e−4. After restricting this set of variants to those implicated in our eQTL analysis at a marginal p value cutoff of 1e−4, we identified 40 associations, where platelet eQTLs were previously linked to CVD by GWASs (Table 1). The genetic variant rs1474868 was identified as the variant most strongly associated with platelet *MFN2* expression levels (p < 1e−47, multiple linear regression; Figure 4) and was the strongest eQTL of all GWAS CVD-linked variants. The variant rs1474868 was previously associated with MI in the STAMPEED: Cardiovascular Health Study (phs000226) and localized to the second intron of the first transcript isoform (GenBank: NM_014874) of *MFN2*. Using our ASE approach, we validated the eQTL association between rs1474868 and *MFN2* expression levels (Figure S5).

Platelet RNA-Seq Data Reveal Unannotated Exon 2b in *MFN2*

MFN2 encodes mitofusin-2, a critical membrane protein involved in mitochondrial fusion, and normal platelet

Table 1. Platelet eQTLs Overlap Variants Implicated in CVD GWASs

SNP	Gene	Gene MIM No.	eQTL p Value	Trait	Study ID
rs1474868	*MFN2*	608507	8.94e−47	myocardial infarction	2873
rs780633	*RSU1*	179555	2.71e−42	stroke	2887
rs2701268	*PDK1*	602524	1.66e−21	stroke	2886
rs7349405	*CLHC1 (C2orf63)*	NA	7.72e−20	hypertension	3041
rs2285515	*FXYD5*	606669	1.96e−19	Behcet syndrome	2888
rs6869332	*ELOVL7*	614451	1.06e−14	stroke	2887
rs6738196	*PDK1*	602524	1.37e−12	stroke	2886
rs3769321	*PDK1*	602524	1.00e−11	stroke	2886
rs514659	*ABO*	110300	2.85e−10	cardiovascular diseases	NA
rs10863938	*LPGAT1*	610473	2.26e−9	stroke	2886
rs10499859	*CD36*	173510	5.12e−9	hypertension	NA
rs712665	*REEP5*	125265	6.46e−9	stroke	2886
rs9962325	*NAPG*	603216	6.47e−9	carotid stenosis	966
rs411356	*REEP5*	125265	8.28e−9	stroke	2886
rs505922	*ABO*	110300	1.60e−8	venous thrombosis	NA
rs505922	*ABO*	110300	1.60e−8	venous thromboembolism	NA
rs4756196	*CD44*	107269	8.27e−8	stroke	2887
rs12242391	*TSPAN15*	613140	3.21e−7	stroke	2887
rs4937126	*ST3GAL4*	104240	3.30e−7	coronary artery disease	NA
rs2522447	*PAPSS1*	603262	7.90e−7	coronary disease	3056
rs102275	*FADS2*	606149	1.69e−6	hypertrophy, left ventricular	3052
rs6935954	*HIST1H2BD*	602799	2.44e−6	stroke	2887
rs102275	*FADS1*	606148	2.77e−6	hypertrophy, left ventricular	3052
rs2980996	*PIGN*	606097	2.81e−6	heart failure	2884
rs174576	*FADS1*	606148	3.54e−6	hypertrophy, left ventricular	3052
rs174576	*FADS2*	606149	3.68e−6	hypertrophy, left ventricular	3052
rs973126	*PAPSS1*	603262	4.38e−6	coronary disease	3056
rs973126	*PAPSS1*	603262	4.38e−6	coronary disease	3055
rs9258966	*HLA-H*	NA	4.42e−6	Behcet syndrome	2888
rs3094654	*HLA-H*	NA	4.42e−6	Behcet syndrome	2888
rs2256919	*ZFP57*	612192	5.73e−6	Behcet syndrome	2888
rs6594646	*REEP5*	125265	6.88e−6	stroke	2886
rs663354	*PIGN*	606097	7.78e−6	heart failure	2884
rs2431512	*REEP5*	125265	8.53e−6	stroke	2886
rs12719151	*REEP5*	125265	1.15e−5	stroke	2886
rs4694656	*CXCL5*	600324	2.18e−5	heart failure	2885
rs13325747	*RPN1*	180470	2.65e−5	heart failure	2885
rs4601174	*CD164*	603356	2.95e−5	heart failure	2885
rs2071653	*ZFP57*	612192	3.91e−5	Behcet syndrome	2888
rs1339965	*SMYD3*	608783	4.58e−5	heart failure	2885

This table contains marginal platelet eQTLs (p < 1e−4) that have been previously associated with CVD. The "Study ID" column contains the study cohort in which the association between SNP and trait was detected. NA stands for "not available."
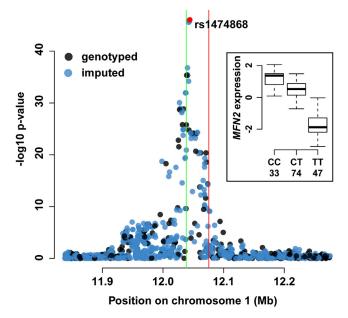
Figure 4. MFN2 eQTL Manhattan Plot
The y and x axes correspond to association p values and genomic coordinates, respectively. Blue and black points show imputed and genotyped variants, respectively. Four variants (points fall on top of each other) were strongly associated with *MFN2* expression levels (p < 1e−45, multiple linear regression), and the red point highlights the eQTL peak rs1474868 (genotyped). Transcription start and stop sites are indicated by green and red vertical lines, respectively.
(Inset) The association between rs1474868 allele dosage and *MFN2* expression levels (significant at p < 1e−47, multiple linear regression). The y and x axes indicate the corrected *MFN2* expression levels and rs1474868 genotype, respectively. Numbers below the genotype labels indicate the number of samples within each group. The box represents the interquartile range, the horizontal line in the box indicates the median, and the whiskers represent 1.5× the interquartile range.

number and function depend on mitochondrial function.[52] Because the presence of a number of transcribed intronic regions was previously noted in human platelets,[53] we hypothesized that platelets might contain uncharacterized transcripts that coincide with our platelet eQTL signals. Motivated by this hypothesis, we analyzed human platelet RNA-seq data from multiple groups[29,40–42] to examine the transcriptional landscape of platelet *MFN2*. A large number of reads mapped to *MFN2* intron 2, overlapping the eQTL peak rs1474868 (Figure 5A and Figure S6). RNA-seq data from mouse platelets[40] lacked reads mapping to this region in the *MFN2* homolog (Figure S7). We hypothesized that this RNA-seq mapping represents the existence of an unannotated human-platelet-expressed exon, which we call "exon 2b." We used RT-PCR of RNA from human platelets to confirm the presence of exon 2b in the *MFN2* transcript (Figure S8), and sequencing of the RT-PCR products revealed a precise exon 2b location (chr1: 12,043,880–12,044,352, hg19). To test whether exon 2b is present in other tissues, we performed in silico cross-tissue analysis. We were unable to identify comparable expression levels

of exon 2b in mRNA-seq data from any of the 69 Epigenome Roadmap sample types queried, suggesting that exon 2b is preferentially expressed in human platelets (Figure 5B).

Exon 2b Is an Alternative Start Site of *MFN2*

To infer how exon 2b fits into the splicing pattern of *MFN2*, we examined RNA-seq junction reads from a total of 45 RNA-seq samples of human platelets. We were unable to detect any reads connecting exon 2b to any upstream exon, suggesting that exon 2b is an alternative 5′ start site. Using the 5′ RACE assay, we verified the presence of two separate platelet *MFN2* isoforms starting at either exon 2b or exon 1 (Figure S9). Next, we estimated the relative abundance of the *MFN2* isoform containing exon 2b. Using junction reads connecting the 5′ border of exon 3 to any upstream exon can unambiguously distinguish between *MFN2* isoforms. A median of 86% of junction reads mapped from the 3′ border of exon 2b to the 5′ border of exon 3, suggesting that exon 2b is included in the pre-dominant platelet *MFN2* isoform (Figure 5C). Moreover, the relative abundance of this *MFN2* isoform was significantly associated with the rs1474868 genotype (p < 1e−6, Spearman's rank correlation; Figure 5D).
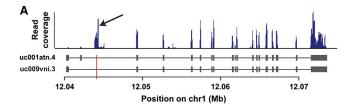
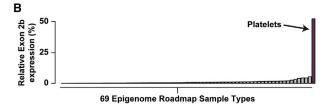### The Variant rs3766744 Alters Transcriptional Activity

eQTLs have been shown to regulate gene expression by altering transcription factor binding sites;[54] therefore, we integrated ENCODE transcription factor ChIP-seq data from K562 myeloid leukemia cells to identify the most likely causal eQTL for *MFN2*. Three noncoding variants (rs4846082, rs4845891, and rs3766744) were in near perfect linkage disequilibrium with rs1474868 and also strongly associated with *MFN2* expression levels (all three p < 1e−45, multiple linear regression). Among this set of variants, we observed an overlap of 32 transcription factor ChIP-seq peaks with rs3766744 (Figure 6A), suggesting a potential mechanism for this variant.

To evaluate the effect of genotype on transcriptional activity, we generated vectors containing short (S: 655 bp) or long (L: 1,928 bp) DNA fragments flanking rs3766744 upstream of a luciferase reporter gene. Clones of the rs37466744 C and T alleles were generated. Transfection of these reporter constructs into K562 cells resulted in a significant difference of luciferase activity between the C and T alleles for both S and L clones (Figure 6B). These results are in concordance with the allelic directionality of our *MFN2* eQTL and ASE findings and support rs3766744 as the causal regulatory variant.

MFN2 Expression Is Associated with Platelet Count

After identifying rs3766744 as the probable causal regulatory variant that controls *MFN2* expression levels, we investigated the association among rs3766744 allele dosage, *MFN2* expression, and platelet count by using our data from the PRAX1 study. Platelet count was significantly associated with rs3766744 allele dosage (p < 1e−4,
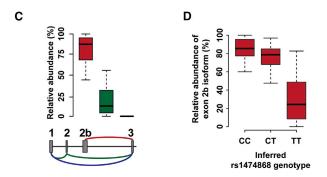
Figure 5. Novel Exon in *MFN2*

(A) Read coverage across *MFN2* for a single representative human platelet RNA-seq sample (SRA: SRR957099). Blue bars represent RNA-seq read coverage. Gray rectangles indicate exons of *MFN2* transcripts uc001atn.4 and uc009vni.3. The black arrow highlights a pile of reads mapping to an intronic region overlapping rs1474868 (red vertical line).

(B) Average exon 2b expression levels across 69 Epigenome Roadmap mRNA-seq sample types (gray bars) and the Londin et al.[29] human platelet RNA-seq data (purple bar). The y axis indicates the exon 2b expression level in relation to that of the most highly expressed *MFN2* exon.

(C) Estimated relative abundances of *MFN2* isoforms in platelets. The schematic below the plot depicts annotated exons 1–3 and novel platelet exon 2b of *MFN2*. Red, green, and blue lines indicate mapping of informative RNA-seq junction reads for the isoform containing the novel exon 2b and annotated *MFN2* isoforms uc001atn.4 and uc009vnl.3, respectively. The boxplot shows the estimated relative abundance for each of these isoforms across human platelet RNA-seq samples. The box represents the interquartile range, the horizontal line in the box indicates the median, and the whiskers represent 1.5× the interquartile range.

(D) Estimated relative abundance of the *MFN2* isoform containing exon 2b by the inferred rs1474868 genotype. The relative abundance of this isoform was significantly associated with the rs1474868 genotype (p < 1e−6, Spearman's rank correlation). The box represents the interquartile range, the horizontal line in the box indicates the median, and the whiskers represent 1.5× the interquartile range.

multiple linear regression; Figure 7A) and *MFN2* expression levels (p < 1e−3, multiple linear regression; Figure 7B). Moreover, after conditioning on *MFN2* expression levels, the association between rs3766744 and platelet count disappeared; however, the association between rs3766744

and *MFN2* expression levels remained significant after platelet count was accounted for. Together, these conditional association analyses support a causal model where *MFN2* expression levels mediate the association between rs3766744 and platelet count (Figure 7C).

Discussion

CVD GWASs have been successful at identifying loci associated with disease risk,[55,56] but linking these variants with gene function in relevant tissues has been a challenge.[16] Platelets are a critical tissue for this analysis because they are an important contributor to clinical CVD phenotypes and are the target of pharmacologic interventions. In this study, we used platelet transcriptomics and eQTL analyses to uncover platelet-specific gene regulation that corresponds to a CVD GWAS signal in *MFN2*. This study demonstrates the power of combining tissue-specific eQTL and RNA-seq data with large-scale genomic databases to gain greater insight into the molecular mechanisms underlying GWAS signals.

Validation of Platelet eQTLs

To corroborate the expression associations revealed in our study, we pursued both overlap with external data and ASE analysis of our own genome-wide genotype and transcriptome data. We utilized imputation to provide a more granular view of the eQTL landscape, enhancing our ability to make direct comparisons to markers in other studies.[57] Second, the imputation approach also determined a more fine-scale substrate for overlap with ChIP-seq analyses. A third benefit of imputation is the improved ability to perform ASE analysis by extending the set of coding variants linked to eQTLs.

We validated eGenes by analyzing allelic imbalance at heterozygous coding sites that had sufficient read coverage and were also in strong linkage disequilibrium with our eQTL peaks.[35] We were able to examine 19% of all platelet eGenes despite the following limitations: (1) only a subset (6.4%) of our cohort was profiled by RNA-seq technology, (2) only a subset (79%) of eGenes contained at least one heterozygous coding site, and (3) only a subset (13%) of pileup sites contained sufficient read coverage for analysis. Globally, the trends indicated a significant concordance between the allelic directionality of eQTLs and RNA-seq allelic-imbalance events in platelet eGenes. Our data suggest that RNA-seq of a subset of subjects for ASE analysis is a useful approach for validating eQTLs developed through microarray studies of gene expression. This approach could be adopted on existing data where microarray studies have determined eQTLs but where subsample RNA-seq could refine candidates for validation and further functional studies.

Characterization of Platelet eQTLs

We integrated and analyzed our primary dataset with GTEx findings to both validate our results and investigate tissue
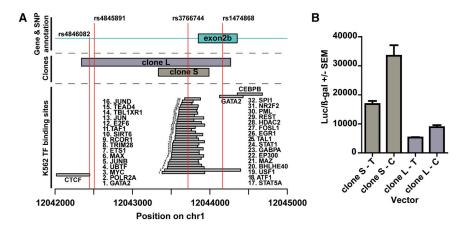
Figure 6. Differential Regulation of *MFN2* Expression by Single-Nucleotide Variant
(A) ENCODE K526 ChIP-seq transcription factor binding peaks clustered near rs1474868. Red vertical lines indicate the location of genetic variants strongly associated with *MFN2* expression levels. rs3766744 overlapped a number of transcription factor binding sites. The names of transcription factors are ordered from bottom to top. Exon 2b is displayed as a cyan rectangle. The S and L clones are shown as purple and gray rectangles, respectively.
(B) Differential luciferase activity for the C and T alleles of rs3766744 in the S and L clones. The luciferase levels were higher for the C allele than for the T allele (both p < 0.05, Mann-Whitney test). Error bars correspond to SE.

specificity of platelet eQTLs. We acknowledge the difficulties of making comparisons across data produced by different groups on different platforms. Our study has the advantage of highly purified cells obtained from living, healthy subjects. Samples from the PRAX1 study were subjected to a uniform and immediate specimen processing, including RNA isolation and extraction within 1 hr of phlebotomy. Our results indicate that platelets have tissue-specific eQTLs distinct from those identified by GTEx, highlighting the need to extend GTEx studies to additional tissues and biological contexts.

Compared to other cell types, platelet eQTL peaks show an unusually high representation in the gene body (Figure 3D). This finding is intriguing because platelets are anucleate cells free of genomic DNA. RNA messages are inherited from parent megakaryocytes, potentially decreasing the relative impact of transcriptional regulatory regions and increasing the significance of post-transcriptional regulation. This stands in sharp contrast to the other cell types profiled in GTEx, where the transcriptome reflects a balance between transcription and RNA degradation. Further analyses of other anucleate cells, such as erythrocytes, might yield additional insights.

Functional Genomics of Platelet *MFN2*
Our genome-wide eQTL analysis revealed that rs1474868 marks the eQTL peak of *MFN2*. The function of *MFN2* in platelets and megakaryocytes has not been studied, and our work demonstrates the presence of *MFN2* transcripts (Figure 5) and protein (Figure S10) in human platelets. *MFN2* is a gene previously reported to function in mitochondrial structure and function.[58,59] Follow-up analyses using RNA-seq data determined that *MFN2* has an unannotated alternate first exon, exon 2b, which overlaps rs1474868. Inclusion of exon 2b is predicted to add 34 amino acids to the N terminus of the MFN2 RefSeq coding sequence; we term this extended protein pMFN2 (Figure S11). The anti-MFN2 antibody used to detect MFN2 does not distinguish between MFN2 and pMFN2. We raised a polyclonal antibody against amino acid

sequence unique to the predicted pMFN2, but unfortunately it reacted non-specifically with numerous polypeptides and was not useful (data not shown). However, because 86% of *MFN2* transcripts contained exon 2b (Figure 5C), we presume the major form observed by western blotting is pMFN2 (Figure S10), but until additional reagents are developed or mass spectrometry of purified pMFN2 is performed, we cannot be certain.

In addition, in silico cross-tissue analysis suggests that this alternate start site is platelet specific. A previous study by Nuernberg et al.[60] identified a novel 5′ start site in RNA-seq data from megakaryocytes in the gene *DNM3*, and we also found this start site in our platelet RNA-seq data (data not shown). Our discovery of an unannotated 5′ alternative start site in platelet *MFN2*, along with similar observations of platelet-specific exons by others,[61] suggests that unannotated lineage-specific alternative 5′ start sites might be common in platelets and platelet progenitor cells. This is an exciting area for further studies.

MFN2 and Platelet Count
We observed a significant association between platelet count and rs3766744, which is in linkage disequilibrium with rs1474868 (Figure 7). Conditional association analysis suggests that this relationship is mediated through differential *MFN2* expression driven by allele dosage. Variant rs3766744 is also in linkage disequilibrium with rs2336384 ($R^2 = 0.49$, LDlink), which has previously been linked to platelet count.[7] We were able to verify this association in our data from the PRAX1 study (p < 0.05, multiple linear regression). However, in the analysis of these data, the association between rs3766744 and platelet count was stronger than the association between rs1474868 and platelet count, suggesting that the platelet-count association might be driven by rs3766744.

Our working hypothesis is that rs3766744 regulates exon 2b utilization by altering transcriptional enhancer activity, which in turn leads to increased *MFN2* expression. Numerous transcription factors were shown to bind to the sequence potentially altered by rs3766744 in K562
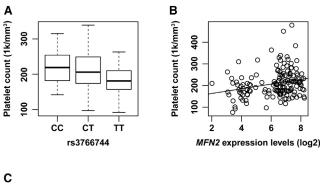
Figure 7. Associations with Platelet Count in the PRAX1 Study Dataset

(A) The association between rs3766744 and platelet count (p < 1e−4, multiple linear regression). The box represents the interquartile range, the horizontal line in the box indicates the median, and the whiskers represent 1.5× the interquartile range.

(B) The association between platelet count and *MFN2* expression levels (p < 1e−3, multiple linear regression).

(C) Our proposed model. The variant rs3766744 controls *MFN2* expression levels, which in turn affect platelet count.

cells (Figure 6A). Particularly interesting candidates are *GATA2*, *TAL1*, and *ETS1*, which are known to regulate megakaryocytopoiesis and expression of many platelet-specific genes. We further hypothesize that variation in *MFN2* expression alters platelet production given that low *Mfn2* expression has been linked to mitochondrial damage in mice,[62] and mitochondrial number and function are critical for platelet production by megakaryocytes. Nevertheless, addressing these testable hypotheses will require much more work and the development of new reagents.

MFN2 and Human Disease

Normal platelet function and lifespan depend on healthy mitochondria as a critical energy source during their 10 day period in circulating blood. There are numerous clinical conditions wherein the platelet count is significantly reduced in association with dysfunctional mitochondria, including inherited and acquired diseases inducing mitochondrial dysfunction.[52,63–67]

Variation in *MFN2* has been linked to Charcot-Marie-Tooth disease (CMT) type 2A2 (MIM: 609260) and hereditary motor and sensory neuropathy VIA (MIM: 601152). *MFN2* mutations are associated with the disease subtype CMT2A, where diverse coding mutations in *MFN2* account for up to 20% of the CMT2A subtype and about 4% of CMT disease overall.[68] The CMT2A-linked mutations in *MFN2* comprise a diverse collection of variants, including stop-gain and non-synonymous pathogenic changes. Pathogenicity has been connected to more variants in the N terminus of the protein, but variations across the protein have been linked to the disease.[69]

Not only does *MFN2* play a role in Mendelian disease, but there is also evidence that *MFN2* might have a function in later-onset complex diseases such as CVD. Common variants in *MFN2* have been linked to platelet count[7] and the risk of MI[25] and hypertension.[70] In addition, mutations in *MFN2* have also been linked to early-onset stroke.[71] Furthermore, it is generally believed that an elevated platelet count is a risk factor for ischemic cardiovascular complications, although this has not been rigorously studied in a prospective fashion. Subjects with very high platelet counts due to acquired, clonal myeloproliferative diseases are at an increased risk of MI and stroke, and standard management most often includes anti-platelet therapies.[72]

Sharing of Results

We have made our results available by extending our interactive Plateletomics website (see Web Resources). We added a platelet-eQTL browser function, allowing users to quickly and easily query our platelet-eQTL results. This eGene analysis can be particularly useful in cases where wet-bench experiments might give conflicting results if the investigator does not consider the genotype of the donors used.

Conclusion

Our study of platelet eQTLs identified 612 platelet eGenes. Among these, *MFN2* harbored the strongest eQTL that corresponded to a previously reported CVD GWAS variant. Integrative analysis demonstrated that the *MFN2* eQTL identified an unannotated alternate platelet-specific 5′ start site driving *MFN2* expression. Moreover, *MFN2* levels were strongly associated with platelet count, a known risk factor for CVD. Our results reinforce using multi-omic data integration of relevant primary tissues to functionalize GWAS signals.

Supplemental Data

Supplemental Data include 11 figures and 4 tables and can be found with this article online at http://dx.doi.org/10.1016/j.ajhg.2016.03.007.

Web Resources

1000 Genomes phase I integrated haplotypes, https://mathgen.stats.ox.ac.uk/impute/data_download_1000G_phase1_integrated_SHAPEIT2.html

AlleleSeq, http://alleleseq.gersteinlab.org/

ArrayExpress, https://www.ebi.ac.uk/arrayexpress/

Cutadapt, https://cutadapt.readthedocs.org/en/stable/

ENCODE, https://www.encodeproject.org/

ENCODE ChIP-seq data on transcription factor binding sites, http://hgdownload.cse.ucsc.edu/goldenpath/hg19/encodeDCC/wgEncodeRegTfbsClustered/wgEncodeRegTfbsClusteredV3.bed.gz

Epigenome Roadmap Project, http://www.roadmapepigenomics.org/

Genboree Workbench, http://genboree.org/site/

Gene Expression Omnibus (GEO), http://www.ncbi.nlm.nih.gov/geo/

GTEx Portal, http://www.gtexportal.org/

IMPUTE2, https://mathgen.stats.ox.ac.uk/impute/impute_v2.html

LDlink, http://analysistools.nci.nih.gov/LDlink

OMIM, http://www.omim.org

Phenotype-Genotype Integrator, http://www.ncbi.nlm.nih.gov/gap/phegeni

Plateletomics, http://www.plateletomics.com/plateletomics/

RefSeq, http://www.ncbi.nlm.nih.gov/refseq/

Sequence Read Archive (SRA), http://www.ncbi.nlm.nih.gov/sra

STAR, https://github.com/alexdobin/STAR

References

1. Chandler, A.B., Chapman, I., Erhardt, L.R., Roberts, W.C., Schwartz, C.J., Sinapius, D., Spain, D.M., Sherry, S., Ness, P.M., and Simon, T.L. (1974). Coronary thrombosis in myocardial infarction. Report of a workshop on the role of coronary thrombosis in the pathogenesis of acute myocardial infarction. Am. J. Cardiol. 34, 823–833.

2. Fuster, V., Badimon, L., Badimon, J.J., and Chesebro, J.H. (1992). The pathogenesis of coronary artery disease and the acute coronary syndromes (2). N. Engl. J. Med. 326, 310–318.

3. Lam, J.Y., Latour, J.G., Lespérance, J., and Waters, D. (1994). Platelet aggregation, coronary artery disease progression and future coronary events. Am. J. Cardiol. 73, 333–338.

4. Davies, M.J., Thomas, A.C., Knapman, P.A., and Hangartner, J.R. (1986). Intramyocardial platelet aggregation in patients with unstable angina suffering sudden ischemic cardiac death. Circulation 73, 418–427.

5. Fitzgerald, D.J., Roy, L., Catella, F., and FitzGerald, G.A. (1986). Platelet activation in unstable coronary disease. N. Engl. J. Med. 315, 983–989.

6. Yee, D.L., Sun, C.W., Bergeron, A.L., Dong, J.F., and Bray, P.F. (2005). Aggregometry detects platelet hyperreactivity in healthy individuals. Blood 106, 2723–2729.

7. Gieger, C., Radhakrishnan, A., Cvejic, A., Tang, W., Porcu, E., Pistis, G., Serbanovic-Canic, J., Elling, U., Goodall, A.H., Labrune, Y., et al. (2011). New gene functions in megakaryopoiesis and platelet formation. Nature 480, 201–208.

8. Bray, P.F. (2007). Platelet hyperreactivity: predictive and intrinsic properties. Hematol. Oncol. Clin. North Am. 21, 633–645, v–vi.

9. Marenberg, M.E., Risch, N., Berkman, L.F., Floderus, B., and de Faire, U. (1994). Genetic susceptibility to death from coronary heart disease in a study of twins. N. Engl. J. Med. 330, 1041–1046.

10. Sørensen, T.I., Nielsen, G.G., Andersen, P.K., and Teasdale, T.W. (1988). Genetic and environmental influences on premature death in adult adoptees. N. Engl. J. Med. 318, 727–732.

11. Rissanen, A.M. (1979). Familial aggregation of coronary heart disease in a high incidence area (North Karelia, Finland). Br. Heart J. 42, 294–303.

12. Lloyd-Jones, D.M., Nam, B.H., D'Agostino, R.B., Sr., Levy, D., Murabito, J.M., Wang, T.J., Wilson, P.W., and O'Donnell, C.J. (2004). Parental cardiovascular disease as a risk factor for cardiovascular disease in middle-aged adults: a prospective study of parents and offspring. JAMA 291, 2204–2211.

13. Bray, P.F., Mathias, R.A., Faraday, N., Yanek, L.R., Fallin, M.D., Herrera-Galeano, J.E., Wilson, A.F., Becker, L.C., and Becker, D.M. (2007). Heritability of platelet function in families with premature coronary artery disease. J. Thromb. Haemost. 5, 1617–1623.

14. Edwards, S.L., Beesley, J., French, J.D., and Dunning, A.M. (2013). Beyond GWASs: illuminating the dark road from association to function. Am. J. Hum. Genet. 93, 779–797.

15. Nica, A.C., and Dermitzakis, E.T. (2013). Expression quantitative trait loci: present and future. Philos. Trans. R. Soc. Lond. B Biol. Sci. 368, 20120362.

16. Battle, A., and Montgomery, S.B. (2014). Determining causality and consequence of expression quantitative trait loci. Hum. Genet. 133, 727–735.

17. Dimas, A.S., Deutsch, S., Stranger, B.E., Montgomery, S.B., Borel, C., Attar-Cohen, H., Ingle, C., Beazley, C., Gutierrez Arcelus, M., Sekowska, M., et al. (2009). Common regulatory variation impacts gene expression in a cell type-dependent manner. Science 325, 1246–1250.

18. Jansen, R.C., and Nap, J.P. (2001). Genetical genomics: the added value from segregation. Trends Genet. 17, 388–391.

19. Westra, H.J., and Franke, L. (2014). From genome to function by studying eQTLs. Biochim. Biophys. Acta 1842, 1896–1902.

20. Schadt, E.E., and Björkegren, J.L. (2012). NEW: network-enabled wisdom in biology, medicine, and health care. Sci. Transl. Med. 4, 115rv1.

21. Goodall, A.H., Burns, P., Salles, I., Macaulay, I.C., Jones, C.I., Ardissino, D., de Bono, B., Bray, S.L., Deckmyn, H., Dudbridge, F., et al.; Bloodomics Consortium (2010). Transcription profiling in human platelets reveals LRRFIP1 as a novel protein regulating platelet function. Blood 116, 4646–4656.

22. Gnatenko, D.V., Dunn, J.J., McCorkle, S.R., Weissmann, D., Perrotta, P.L., and Bahou, W.F. (2003). Transcript profiling of human platelets using microarray and serial analysis of gene expression. Blood 101, 2285–2293.

23. GTEx Consortium (2015). Human genomics. The Genotype-Tissue Expression (GTEx) pilot analysis: multitissue gene regulation in humans. Science 348, 648–660.

24. Raney, B.J., Cline, M.S., Rosenbloom, K.R., Dreszer, T.R., Learned, K., Barber, G.P., Meyer, L.R., Sloan, C.A., Malladi, V.S., Roskin, K.M., et al. (2011). ENCODE whole-genome data in the UCSC genome browser (2011 update). Nucleic Acids Res. 39, D871–D875.

25. Ramos, E.M., Hoffman, D., Junkins, H.A., Maglott, D., Phan, L., Sherry, S.T., Feolo, M., and Hindorff, L.A. (2014). Phenotype-Genotype Integrator (PheGenI): synthesizing genome-wide association study (GWAS) data with existing genomic resources. Eur. J. Hum. Genet. 22, 144–147.

26. Edelstein, L.C., Simon, L.M., Montoya, R.T., Holinstat, M., Chen, E.S., Bergeron, A., Kong, X., Nagalla, S., Mohandas, N., Cohen, D.E., et al. (2013). Racial differences in human

platelet PAR4 reactivity reflect expression of PCTP and miR-376c. Nat. Med. *19*, 1609–1616.

27. Edelstein, L.C., Simon, L.M., Lindsay, C.R., Kong, X., Teruel-Montoya, R., Tourdot, B.E., Chen, E.S., Ma, L., Coughlin, S., Nieman, M., et al. (2014). Common variants in the human platelet PAR4 thrombin receptor alter platelet function and differ by race. Blood *124*, 3450–3458.

28. Simon, L.M., Edelstein, L.C., Nagalla, S., Woodley, A.B., Chen, E.S., Kong, X., Ma, L., Fortina, P., Kunapuli, S., Holinstat, M., et al. (2014). Human platelet microRNA-mRNA networks associated with age and gender revealed by integrated plateletomics. Blood *123*, e37–e45.

29. Londin, E.R., Hatzimichael, E., Loher, P., Edelstein, L., Shaw, C., Delgrosso, K., Fortina, P., Bray, P.F., McKenzie, S.E., and Rigoutsos, I. (2014). The human platelet: strong transcriptome correlations among individuals associate weakly with the platelet proteome. Biol. Direct *9*, 3.

30. Engström, P.G., Steijger, T., Sipos, B., Grant, G.R., Kahles, A., Rätsch, G., Goldman, N., Hubbard, T.J., Harrow, J., Guigó, R., and Bertone, P.; RGASP Consortium (2013). Systematic evaluation of spliced alignment programs for RNA-seq data. Nat. Methods *10*, 1185–1191.

31. Shabalin, A.A. (2012). Matrix eQTL: ultra fast eQTL analysis via large matrix operations. Bioinformatics *28*, 1353–1358.

32. Stegle, O., Parts, L., Durbin, R., and Winn, J. (2010). A Bayesian framework to account for complex non-genetic factors in gene expression levels greatly increases power in eQTL studies. PLoS Comput. Biol. *6*, e1000770.

33. Howie, B.N., Donnelly, P., and Marchini, J. (2009). A flexible and accurate genotype imputation method for the next generation of genome-wide association studies. PLoS Genet. *5*, e1000529.

34. Degner, J.F., Marioni, J.C., Pai, A.A., Pickrell, J.K., Nkadori, E., Gilad, Y., and Pritchard, J.K. (2009). Effect of read-mapping biases on detecting allele-specific expression from RNA-sequencing data. Bioinformatics *25*, 3207–3212.

35. Castel, S.E., Levy-Moonshine, A., Mohammadi, P., Banks, E., and Lappalainen, T. (2015). Tools and best practices for data processing in allelic expression analysis. Genome Biol. *16*, 195.

36. Rozowsky, J., Abyzov, A., Wang, J., Alves, P., Raha, D., Harmanci, A., Leng, J., Bjornson, R., Kong, Y., Kitabayashi, N., et al. (2011). AlleleSeq: analysis of allele-specific expression and binding in a network framework. Mol. Syst. Biol. *7*, 522.

37. Hinrichs, A.S., Karolchik, D., Baertsch, R., Barber, G.P., Bejerano, G., Clawson, H., Diekhans, M., Furey, T.S., Harte, R.A., Hsu, F., et al. (2006). The UCSC Genome Browser Database: update 2006. Nucleic Acids Res. *34*, D590–D598.

38. Harvey, C.T., Moyerbrailean, G.A., Davis, G.O., Wen, X., Luca, F., and Pique-Regi, R. (2015). QuASAR: quantitative allele-specific analysis of reads. Bioinformatics *31*, 1235–1242.

39. Li, H., Handsaker, B., Wysoker, A., Fennell, T., Ruan, J., Homer, N., Marth, G., Abecasis, G., and Durbin, R.; 1000 Genome Project Data Processing Subgroup (2009). The Sequence Alignment/Map format and SAMtools. Bioinformatics *25*, 2078–2079.

40. Rowley, J.W., Oler, A.J., Tolley, N.D., Hunter, B.N., Low, E.N., Nix, D.A., Yost, C.C., Zimmerman, G.A., and Weyrich, A.S. (2011). Genome-wide RNA-seq analysis of human and mouse platelet transcriptomes. Blood *118*, e101–e111.

41. Kissopoulou, A., Jonasson, J., Lindahl, T.L., and Osman, A. (2013). Next generation sequencing analysis of human platelet PolyA+ mRNAs and rRNA-depleted total RNA. PLoS ONE *8*, e81809.

42. Eicher, J.D., Wakabayashi, Y., Vitseva, O., Esa, N., Yang, Y., Zhu, J., Freedman, J.E., McManus, D.D., and Johnson, A.D. (2016). Characterization of the platelet transcriptome by RNA sequencing in patients with acute myocardial infarction. Platelets *27*, 230–239.

43. Coarfa, C., Pichot, C., Jackson, A., Tandon, A., Amin, V., Raghuraman, S., Paithankar, S., Lee, A.V., McGuire, S.E., and Milosavljevic, A. (2014). Analysis of interactions between the epigenome and structural mutability of the genome using Genboree Workbench tools. BMC Bioinformatics *15* (*Suppl 7*), S2.

44. Nagalla, S., Shaw, C., Kong, X., Kondkar, A.A., Edelstein, L.C., Ma, L., Chen, J., McKnight, G.S., López, J.A., Yang, L., et al. (2011). Platelet microRNA-mRNA coexpression profiles correlate with platelet reactivity. Blood *117*, 5189–5197.

45. Hasin-Brumshtein, Y., Hormozdiari, F., Martin, L., van Nas, A., Eskin, E., Lusis, A.J., and Drake, T.A. (2014). Allele-specific expression and eQTL analysis in mouse adipose tissue. BMC Genomics *15*, 471.

46. Majewski, J., and Pastinen, T. (2011). The study of eQTL variations by RNA-seq: from SNPs to phenotypes. Trends Genet. *27*, 72–79.

47. Holm, T., Damås, J.K., Holven, K., Nordøy, I., Brosstad, F.R., Ueland, T., Währe, T., Kjekshus, J., Frøland, S.S., Eiken, H.G., et al. (2003). CXC-chemokines in coronary artery disease: possible pathogenic role of interactions between oxidized low-density lipoprotein, platelets and peripheral blood mononuclear cells. J. Thromb. Haemost. *1*, 257–262.

48. Labelle, M., Begum, S., and Hynes, R.O. (2014). Platelets guide the formation of early metastatic niches. Proc. Natl. Acad. Sci. USA *111*, E3053–E3061.

49. Ren, Q., Wimmer, C., Chicka, M.C., Ye, S., Ren, Y., Hughson, F.M., and Whiteheart, S.W. (2010). Munc13-4 is a limiting factor in the pathway required for platelet granule release and hemostasis. Blood *116*, 869–877.

50. Feldmann, J., Callebaut, I., Raposo, G., Certain, S., Bacq, D., Dumont, C., Lambert, N., Ouachée-Chardin, M., Chedeville, G., Tamary, H., et al. (2003). Munc13-4 is essential for cytolytic granules fusion and is mutated in a form of familial hemophagocytic lymphohistiocytosis (FHL3). Cell *115*, 461–473.

51. Lafuente, E.M., van Puijenbroek, A.A., Krause, M., Carman, C.V., Freeman, G.J., Berezovskaya, A., Constantine, E., Springer, T.A., Gertler, F.B., and Boussiotis, V.A. (2004). RIAM, an Ena/VASP and Profilin ligand, interacts with Rap1-GTP and mediates Rap1-induced adhesion. Dev. Cell *7*, 585–595.

52. Leaver, H.A., Schou, A.C., Rizzo, M.T., and Prowse, C.V. (2006). Calcium-sensitive mitochondrial membrane potential in human platelets and intrinsic signals of cell death. Platelets *17*, 368–377.

53. Bray, P.F., McKenzie, S.E., Edelstein, L.C., Nagalla, S., Delgrosso, K., Ertel, A., Kupper, J., Jing, Y., Londin, E., Loher, P., et al. (2013). The complex transcriptional landscape of the anucleate human platelet. BMC Genomics *14*, 1.

54. Castaldi, P.J., Cho, M.H., Zhou, X., Qiu, W., Mcgeachie, M., Celli, B., Bakke, P., Gulsvik, A., Lomas, D.A., Crapo, J.D., et al. (2015). Genetic control of gene expression at novel and established chronic obstructive pulmonary disease loci. Hum. Mol. Genet. *24*, 1200–1210.

55. Smith, J.G., and Newton-Cheh, C. (2015). Genome-wide association studies of late-onset cardiovascular disease. J. Mol. Cell. Cardiol. *83*, 131–141.

56. Roberts, R. (2014). Genetics of coronary artery disease. Circ. Res. *114*, 1890–1903.

57. Porcu, E., Sanna, S., Fuchsberger, C., and Fritsche, L.G. (2013). Genotype imputation in genome-wide association studies. Curr. Protoc. Hum. Genet. *Chapter 1*, 25.

58. Chen, H., Chomyn, A., and Chan, D.C. (2005). Disruption of fusion results in mitochondrial heterogeneity and dysfunction. J. Biol. Chem. *280*, 26185–26192.

59. Eura, Y., Ishihara, N., Yokota, S., and Mihara, K. (2003). Two mitofusin proteins, mammalian homologues of FZO, with distinct functions are both required for mitochondrial fusion. J. Biochem. *134*, 333–344.

60. Nürnberg, S.T., Rendon, A., Smethurst, P.A., Paul, D.S., Voss, K., Thon, J.N., Lloyd-Jones, H., Sambrook, J.G., Tijssen, M.R., Italiano, J.E., Jr., et al.; HaemGen Consortium (2012). A GWAS sequence variant for platelet volume marks an alternative DNM3 promoter in megakaryocytes near a MEIS1 binding site. Blood *120*, 4859–4868.

61. Schubert, S., Weyrich, A.S., and Rowley, J.W. (2014). A tour through the transcriptional landscape of platelets. Blood *124*, 493–502.

62. Chen, W., Xu, X., Wang, L., Bai, G., and Xiang, W. (2015). Low Expression of Mfn2 Is Associated with Mitochondrial Damage and Apoptosis of Ovarian Tissues in the Premature Ovarian Failure Model. PLoS ONE *10*, e0136421.

63. Illsinger, S., Janzen, N., Sander, S., Schmidt, K.H., Bednarczyk, J., Mallunat, L., Bode, J., Hagebölling, F., Hoy, L., Lücke, T., et al. (2010). Preeclampsia and HELLP syndrome: impaired mitochondrial function in umbilical endothelial cells. Reprod. Sci. *17*, 219–226.

64. Yen, H.H., Shih, K.L., Lin, T.T., Su, W.W., Soon, M.S., and Liu, C.S. (2012). Decreased mitochondrial deoxyribonucleic acid and increased oxidative damage in chronic hepatitis C. World J. Gastroenterol. *18*, 5084–5089.

65. Pereira, J., Soto, M., Palomo, I., Ocqueteau, M., Coetzee, L.M., Astudillo, S., Aranda, E., and Mezzano, D. (2002). Platelet aging in vivo is associated with activation of apoptotic pathways: studies in a model of suppressed thrombopoiesis in dogs. Thromb. Haemost. *87*, 905–909.

66. Yamada, K., Miwa, K., Wakita, Y., Ikoma, Y., Fukui, Y., Okuyama, M., Kato, K., Ichihashi, T., Kunishima, S., and Shamoto, M. (1995). Familial macrothrombocytopenia with unusually elongated mitochondria. Intern. Med. *34*, 1140–1143.

67. White, J.G., Key, N.S., King, R.A., and Vercellotti, G.M. (2004). The White platelet syndrome: a new autosomal dominant platelet disorder. Platelets *15*, 173–184.

68. Fridman, V., Bundy, B., Reilly, M.M., Pareyson, D., Bacon, C., Burns, J., Day, J., Feely, S., Finkel, R.S., Grider, T., et al.; Inherited Neuropathies Consortium (2015). CMT subtypes and disease burden in patients enrolled in the Inherited Neuropathies Consortium natural history study: a cross-sectional analysis. J. Neurol. Neurosurg. Psychiatry *86*, 873–878.

69. DiVincenzo, C., Elzinga, C.D., Medeiros, A.C., Karbassi, I., Jones, J.R., Evans, M.C., Braastad, C.D., Bishop, C.M., Jaremko, M., Wang, Z., et al. (2014). The allelic spectrum of Charcot-Marie-Tooth disease in over 17,000 individuals with neuropathy. Mol. Genet. Genomic Med. *2*, 522–529.

70. Wang, Z., Liu, Y., Liu, J., Liu, K., Wen, J., Wen, S., and Wu, Z. (2011). HSG/Mfn2 gene polymorphism and essential hypertension: a case-control association study in Chinese. J. Atheroscler. Thromb. *18*, 24–31.

71. Chung, K.W., Cho, S.Y., Hwang, S.J., Kim, K.H., Yoo, J.H., Kwon, O., Kim, S.M., Sunwoo, I.N., Züchner, S., and Choi, B.O. (2008). Early-onset stroke associated with a mutation in mitofusin 2. Neurology *70*, 2010–2011.

72. Campbell, P.J., and Green, A.R. (2005). Management of polycythemia vera and essential thrombocythemia. Hematology (Am Soc Hematol Educ Program) *2005*, 201–208.